Model Predictive Control Strategy-Based Voltage Sensing of Quasi Z-Source Cascaded Multi-Level PV Inverter with Distributed MPPT Algorithm

M. Senthil Kumar*, J. Vishnupriyan**, Nallapaneni Manoj Kumar ***‡

*Department of Electrical and Electronics Engineering, KIT & KIM Technical Campus, Karaikudi-630307, Tamil Nadu, India

**Department of Electrical and Electronics Engineering, Chennai Institute of Technology, Kundrathur, Chennai-600069, Tamil Nadu, India

***School of Energy and Environment, City University of Hong Kong, Kowloon, Hong Kong

(masansenthil@gmail.com; vishnupriyanj@gmail.com; nallapanenichow@gmail.com)

‡ Corresponding Author; Nallapaneni Manoj Kumar, School of Energy and Environment, City University of Hong Kong, Kowloon, Hong Kong., Tel: +852 68455883, nallapanenichow@gmail.com; mnallapan2-c@my.cityu.edu.hk

Received: 06.01.2020 Accepted:18.02.2020

Abstract- The evolving quasi Z-source cascaded multilevel inverters (QZS-CMI) need appropriate control logic for effective switching state of operation. This work proposes the model predictive control (MPC) based QZS-CMI in a PV generation system. The MPC, with its characteristic of prediction of future response and efficient constraint handling capacity, controls the output voltage and capacitor voltage. The proposed topology effectively solves the significant detrimental aspect of switching stress, usually arising in a high voltage inverter system by the increased number of levels of the inverter circuit. The MPC based control strategy exhibits a fast-dynamic response and maintains the output power quality in an off-grid application. The simulation model with experimental results helps to validate the optimal operation of the proposed control logic in seven levels QZS-CMI.

Keywords Cascaded multilevel inverter, quasi Z-source, voltage sensing, model predictive control, solar power system, distributed PV power, PV array.

Nomenclature

$i(k+1)$	predicted current vector
$V_{C1n}(k)$	instantaneous sampling voltage vector
T_s	sampling time
L_f	filter inductance
R_f	filter resistance
R_l	resistance of the filter inductor
e	load voltage
$V_0(k+1)$	predicted output voltage vector
i(k)	current vector
V_{mpp*}	maximum power point reference voltage vector

1. Introduction

The solar photovoltaic (PV) electricity generation is one of the promising options, as solar radiation is in abundance. PV panel has its own drawbacks of reduced efficiency and partial shading [1]. Other reasons like variable wind speeds, humidity, low light level and cell temperature variations also effects [2]. Therefore, it is necessary to track continuously maximum power point (MPP) in order to maximize the power output from a PV system for a given set of operating conditions. Multilevel inverters are widely used in the integration of the PV system with the isolated load/grid [3]. Cascaded multilevel inverter (CMI) is more advantageous in recent days due to its modular structure [4]. In this case, the rating of CMI should be higher even for lower PV voltage. Here a DC-link imbalance problem [5].

A two-stage inverter solves the arising problems with the step-up converter in each module [6]. The two-stage inverter requires many components that make the system more complex and increase the losses. The component loss can be reduced by quasi Z-source cascaded multilevel inverter (QZS-CMI), which operates on the same principle of CMI [7], whereas it is designed as a single-stage inverter. In [8] a single-phase extended-boost quasi-Z source (EqZS) cascaded multilevel inverter (CMI) for photovoltaic power systems is proposed. The QZS-CMI utilizes only one-third of the modules and exhibits elevated detrimental effects.

Control of the converter is an effective way to achieve the desired performance of power converters. Some of the control strategies, which are involved in multilevel inverters, are Current hysteresis control (CHC), proportional-integral (PI) control, and proportional-resonant (PR) control. The literature does not have sufficient reports on MPC based single phase 7-level QZS-CMI with solar PV based power system. MPC based voltage sensing of QZS-CMI of PV power generation system is proposed in this work. The performance analysis is carried out in terms of dynamic response and load current THD with source-side disturbances. The implemented scheme can effectively be used for solar heaters, water pumps, battery chargers, electric vehicles, home electrification, PV for irrigations.

This paper is organized as follows. Section 2 Literature review and contribution of the work is described. The basic principle of quasi Z-source cascaded multilevel inverters is explained in Section 3. Control schemes such as MPPT and MPC algorithms are analysed in Section 4. The performance of the proposed system is compared with the existing system through simulation in the MATLAB SIMULINK environment. Simulation results show the superiority of the proposed system, and the system is verified experimentally with a 450W solar panel in Section 5. Section 6 summarizes the conclusions and future work.

2. Literature Review

ZSI and QZSI could achieve voltage buck/ boosting with a single-stage converter topology, thus overcome the range limitation of output voltage gain [9]. The battery-assisted qZSI can balance the stochastic fluctuations of the wind power injected to the load and improve the voltage and frequency control [10]. In [11] a comparative analysis of different levels of QSZ-CMI inverter with respect to voltage gain and THD is done.

In [12] the characteristics of slide mode and PR control, a cascaded controller is proposed for bipolar single-phase uninterruptible power supply (UPS) inverter. The non-linear sliding mode control is applied on ship-roll stabilization problem and frequency regulation in power system to improve the system dynamic performance in terms of low overshoot and reduced settling time [13].

The development of the model predictive control (MPC) scheme dates back to late seventies when it was first applied in chemical process industries. The term MPC does not describe a specific control technique but it includes a wide range of control methods and implementation. The application of MPC strategy in the area of electrical drives and PEC is more recent [14].MPC has demonstrated to offer a very simple and effective alternative to classical control algorithms with Pulse Width Modulation (PWM) for controlling the flow of electrical energy using power converters [15]. In [16] analysis, design, and implementation of a digital predictive current control technique known as model predictive current controller for the control of single phase power inverter integrating renewable energy based plant with the grid. Finite control set model predictive control by using a constant switching operation for a boost converter connected to a PV panel. The proposal is an alternative for a finite control set model predictive control that operates without constant switching operation [17].An auto adaptive discrete-time model predictive control (ADMPC) system is based on the optimization of an objective function that considers the reference and the real speed as well as the acceleration of the IM drive by using the state-space model in [18].

3. Quasi Z-source Cascaded Seven Level Inverter

A separate PV panel, which includes DC source, is required for each bridge in series cascaded single-phase quasi Z-source H-bridges inverter. Moreover, to balance the fluctuations of PV power injected to the load, the system uses a battery in each module. In the circuits of the selected model, PV array and QZS network capacitors are charging, when the inductors are at shoot-through states. The topology of the proposed system is shown in Fig. 1. The resulting output voltage is combined with the addition of the voltage waveform generated by the individual module. The output voltage levels are generated by 2n+1, where n is the number of modules. It operates in two modes:

- Mode 1: non-shoot-through states;
- Mode 2: In shoot-through states.

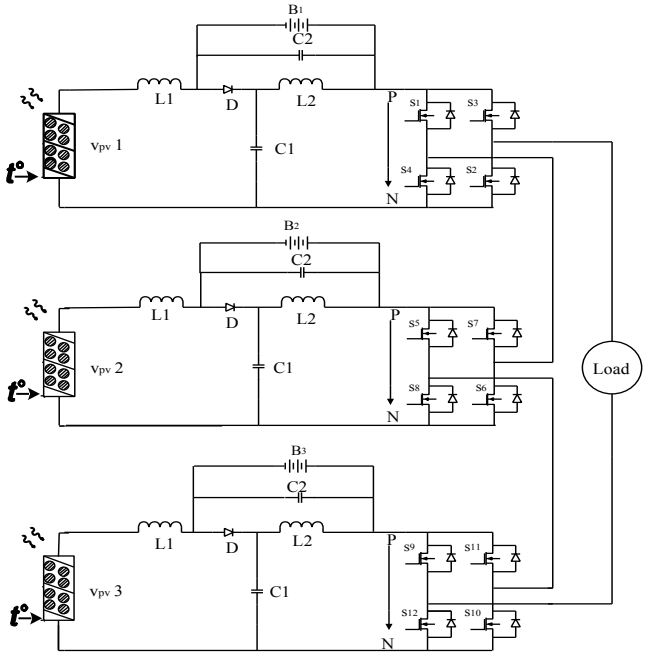

Fig. 1. The topology of the 7-level QSZ-CM

3.1. Shoot-through state (Non-active mode)

At shoot-through state, input voltage and QZS capacitors charge inductors, and qZS diode is cut off because of negative voltage. In this mode, switches of the same phase in the inverter bridge are switched on simultaneously for a very short duration. The source, however, does not get short-circuited, when it is attempted to do so because of the presence LC network while boosting the output voltage. A boost factor boosts the DC-link voltage during the shoot-through states, and whose value depends on the shoot-through duty ratio for a given modulation index.

3.2. Non-shoot through the state (Active mode)

In the non-shoot-through mode, the switching pattern of the QZSI is similar to that of a voltage source inverter (VSI). The inverter bridge viewed from the DC side is equivalent to a current source. The input DC voltage is available as DC-link voltage input to the inverter, and it makes the QZSI behave similarly to a VSI.

The n^{th} module battery current and the power are meet the below relationship with its inductor currents and power of the PV system.

The energy storage of the qZS module performs the following process:

- The battery will discharge,

  Conditions: Ppvn < Pn, Pbn > 0, ibn > 0;
- The battery will charge,

  Conditions: Ppvn > Pn, Pbn < 0, ibn < 0;
- The battery will neither discharge nor charge,

  Conditions: Ppvn = Pn, Pbn = 0, ibn =0.

4. Control Schemes

4.1. Maximum Power Point Control

Generally, voltage and current are measured for manipulating maximum power point tracking. The proposed method has the advantage of measuring only voltage for manipulating the maximum power for the PV panel. The input resistance Rin of the inverter acts as load resistance for the PV module. When the load resistance matches the internal resistance of the source (solar array) at any given irradiation, then Maximum power transfer is possible. By varying the duty cycle, the effective load resistance *(R)* is varied and is given by Eq. (1).

$$R_{in} = \frac{V_{in}}{I_{in}} = \left(\frac{1-D}{D}\right)^2 \frac{V_0}{I_0} = \left(\frac{1-D}{D}\right)^2 R \tag{1}$$

The PV module power, as given in Eq. (2).

$$P_{pv} = V_{pv} I_{pv} = P_{pv} = V_{pv} \frac{V_{pv}}{R_{in}} \tag{2}$$

By substituting R_{in} from the Eq. (1) in Eq. (2), the PV module power becomes as shown in Eq. (3).

$$P_{pv} = V_{pv} \frac{V_{pv}}{\left(\left(\frac{1-D}{D}\right)^2 R\right)} \tag{3}$$

Considering that many converters are connected in series, the voltage change forced by one cell generates only a minor variation in the load current. If the load current for each converter can be assumed as a constant, then the output power of each individual converter is proportional to its output voltage. The MPPT function can be achieved by sensing and maximizing the output voltage. This approach is valid for any case where an increase in converter output voltage produces a monotonic, but not necessarily proportional, increase in load power. The output voltage can be determined from the cell voltage and the converter duty cycle. A simple perturb and observe scheme is employed to track the peak power. From Eq. (3) by changing the duty cycle *(D)* of the inverter, the load resistance of the PV panel is improved in such a way that the PV module will produce maximum power at any irradiation level and temperature condition.

4.2. Model predictive controller

The direct power control of the MPC controller tracks instantaneous power and operates under non-linear condition. Besides, MPC is easy to implement, and it also provides flexibility while incorporating various other variables and their constraints without disturbing the main control design [19]. MPC scheme operates with two main layers, and they are predictive model and cost function optimization. The future behaviors of the control variables are predicted by the discrete-time dynamic model of the system [20,21]. The cost function minimizes the error between the references and future control variable in the next sampling time.

4.2.1. Models of the system

The system variable of QZS-CMI *(x_k)* and the output voltage is measured. The predictive model calculates future values. By relating the measured value with future values, the closest value of reference value is selected. The corresponding control action is generating pulse to the switches of the QZS-CMI. Then set future value *(k=k+1),* and the steps are repeated.

The dynamics of the load is designated by the vector Eq. (4)

$$v = L\frac{di}{dt} + (R + R_L)i + e \tag{4}$$

4.2.2. Discrete-Time models of the system

The inverter output voltage *(V_o)* and capacitor voltage *(V_{CIn})* controlled by two discrete-time dynamic models; it can be formed from the continuous-time variables. In order

to obtain the dynamic models of the system, the Euler equation is used to calculate the differential equations of the capacitor voltage and the load voltage.

$$\frac{df}{dt} \approx \frac{f(x_0 + h) - f(x_0)}{h} \tag{5}$$

The next sampling time is calculated from the Eq. (5), it has been changed as discretization

$$\frac{\Delta f(k)}{\Delta t} \approx \frac{f(k+1) - f(k)}{T_s} \tag{6}$$

The predictive model of the QZS-CMI I: This model is employed to predict the forthcoming behavior of output voltage *(V_o)* from the individual bridge. Eq. (6) substitute into Eq. (4), the output voltage of the discrete-time model is

$$v_o(k+1) = v(k+1) - R_L i(k+1) - L\frac{i(k+1) - i(k)}{Ts} \tag{7}$$

The predictive model of the QZS-CMI II: To stabilize the inverter system the QZS network inductor current and capacitor voltage is regulated. This regulation is succeeded by adding cost function and description equation. Suppose network inductors *L1=L2,* and capacitors *C1=C2* for a balanced network, $x = 1,2$:

$$g_C = \left| v^*_{capx} - v_{capx}(k+1) \right| \tag{8}$$

The next step capacitor voltage *(V_{cap})* reference value is calculated by

$$v^*_{capx} = 2 * v^p_{out} \tag{9}$$

At the shoot-through state and non-shoot-through state, the ration between modulation index *M* and shoot-through ratio *D* is one, and *Vcapx(k+1)* is the future capacitor voltage, it has been estimated by shoot-through and non-shoot-through state.

During non-shoot through the case, the diode is turned on. The inductor voltage and the capacitor current at this case can be expressed as

$$v_{capx}(k+1) = v_{capx}(k) + \frac{T_s}{C_{capx}}(i_{indx}(k+1) - i_{inv}(k+1)) \tag{10}$$

where $i_{inv}(k+1)$ is the inverter output current that can be formulated as a function of the switching state also with simplifying the derivative term as present in the future current.

During shoot-through case the diode is being in reverse biasing, and the following equation for inductor voltage and capacitor current can be obtained

$$v_{capx}(k+1) = v_{capx}(k) - \frac{T_s}{C_{capx}} i_{indx}(k+1) \tag{11}$$

where C_{capx} is the capacitor capacitance, $i_{indx}(k+1)$ is the future inductor current; it is approximated to be $i_{indx}(k)$ for an appropriate sampling time $i_{inv}(k+1)$ is the inverter current, it is estimated from the load measurement.

4.2.3. Cost function optimization

The cost function of the MPC control strategy is framed using the reference value from the MPPT algorithm. This MPPT algorithm tracks the maximum value of productive output and gives out an appropriate duty cycle. The predictive model and the MPPT reference values together constitute the calculation of cost function, and it is almost optimum. Fig. 2 shows the block diagram of the proposed system.

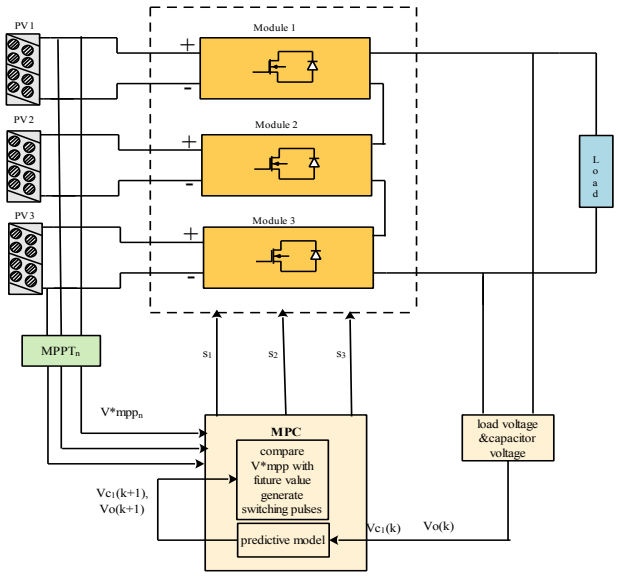

Fig. 2. Block diagram of the model predictive control method

The output voltage cost function is derived by

$$g_i = \left\| v^*_{n\,mpp}(k+1) - v_o(k+1) \right\|^2 \tag{12}$$

Active states of the QZSI are kept the same as in VSI to avoid extinguishing the waveform of the output voltage, and the boosting feature is achieved using the shoot-through duty cycle within the traditional zero states. Therefore, the possible switching states for the considerable converter are eight states which are seven states at a non-shoot-through case and one state at the shoot-through case. The output of the inverter across the terminals of the load varies with these states of the converter.

4.3. Control Algorithm

The flowchart is shown in Fig. 3. illustrates the flow of the proposed MPC control methodology. The optimization control algorithm is implemented to minimize the cost function for a number of cycles repeatedly. It finds the minimum value of cost function, which could be stored along with the index value of the equivalent switching pulse generation.

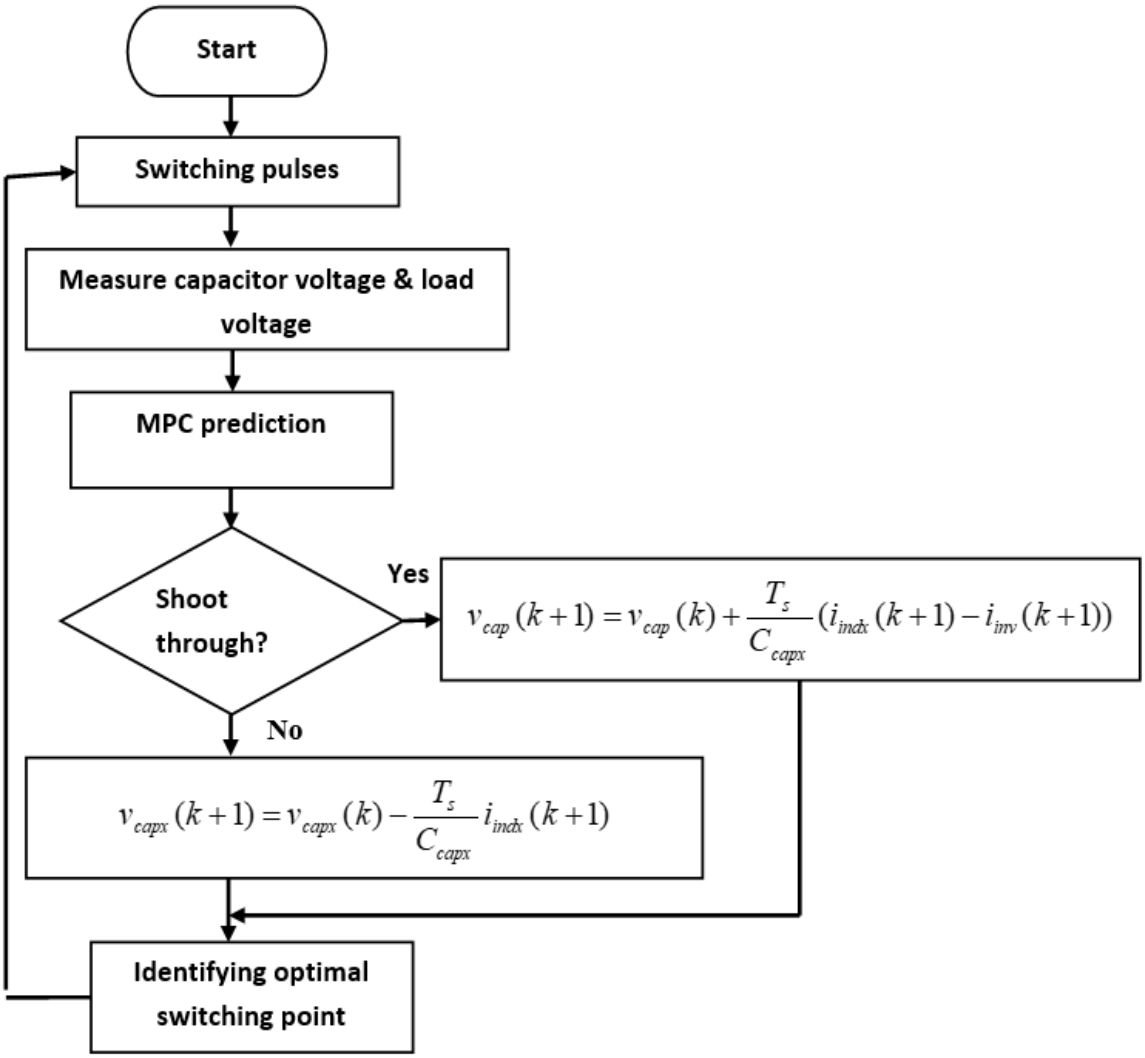

Fig. 4. DC link voltages of the bridge module 1, 2 & 3

The control algorithm can be summarized by Sampling the output voltage, capacitors voltage. These are used to predict output voltage and capacitor voltage using the predictive model I and predictive model II respectively. All prediction is evaluated using the cost function. The optimal switching state that corresponds to the optimal voltage vector that minimizes the cost function is selected to be applied at the next sampling time.

5. Results and Discussion

5.1. Simulation Results

An identical 50V PV panel connected with QZS-CMI modules for standalone mode is designed to verify the proposed technique. The specifications of a solar module Sukam 150W specification is given in Table 1. In the developed PV model, the irradiation level is varied, and the temperature is constant (25ºC). Simulation of the system is carried out through MATLAB, and the results are taken. The system power is approximately (3X150W) 450 W with a 12V battery in the individual system module. The system specifications for simulations are listed in Table 2.

Table 1. Photovoltaic module parameters

Parameter	Value with units
Maximum power	150 W
Open circuit voltage	22.5 V
Short circuit current	8.75 A
Voltage at the maximum power	18.25 V
Current at the maximum power	8.22 A

Table 2. System specifications

Parameter	Value with units
Input PV voltage	50-100 V
Output load voltage	71 V
QZS inductance	500 µH
QZS capacitance	300 µH
Load resistance	30 Ω
L_f	1 mH
C_f	50 µF

5.1.1. Distributed MPPT Control Analysis

Panel 1: 800 W/m2 and 50° C, Vpv = 15V.

For the first panel, the PV voltage is 15 V, to achieve 24 V for first bridge output voltage, the modulation index can be calculated by the below equation, which is the inverse:

$$M = \frac{2\hat{v}_o}{4\hat{v} - V_{pv}} = \frac{2 \times 24}{4 \times 24 - 15} = 0.6$$

The boost factor is $B = \frac{1}{2M - 1} = 2.63$

Thus, the shoot-through duty cycle $\frac{T_o}{T} = 1 - m = 0.4$

The capacitor voltage is $V_C = \frac{1 - T_o / T}{1 - 2T_o / T} V_{pv} = 41V$

Panel 2: 700 W/m^2 and 30° C, V_{pv} = 12V

For the second panel, the PV voltage is 12 V; to achieve 24 V for the second bridge output voltage, the modulation index is 0.57. The boost factor is 3.51, and the capacitor voltage is 45.49 V

Panel 3: 900 W/m^2 and 41° C, V_{pv} = 24 V

For the third panel, the PV panel generates 36V it is satisfied with the desired bridge voltage, hence this panel no need to boost the DC link voltage and the modulation index is 0.78.

In all the above cases, the timescale for waveforms of the output voltage, load current in simulations is 0.5 - 1 ms. The input current is continuous, and hence, it will significantly reduce the input stress.

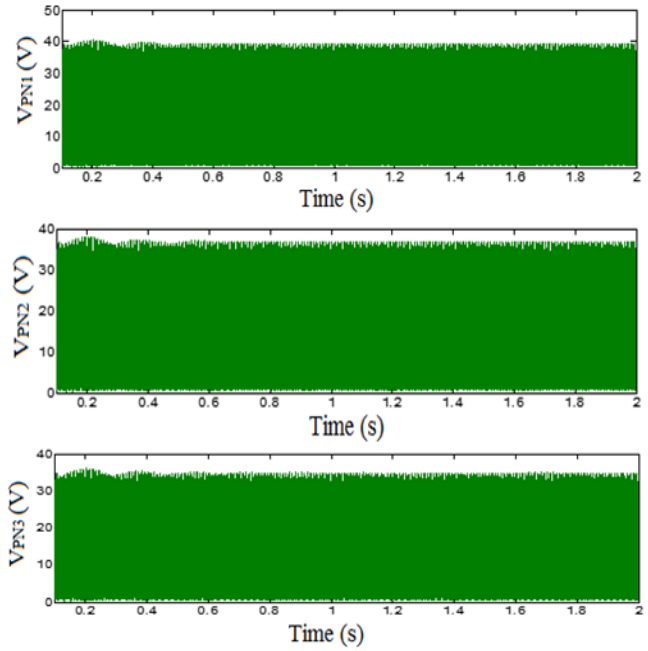

Fig. 4. DC link voltages of the bridge module 1, 2 & 3

The simulated result provides similar results of the existing result even without the modulation technique.

Fig. 4 shows the DC link voltage of the three modules. Table 3. shows the comparison of the DC-link between the theoretical and simulation results.

Figs. 5. & 6 show the capacitor voltages and inductor currents of three modules. Figs 7-9 show the result of seven-level staircase voltage, single-phase load voltage, and load current when the QZS-CMI is controlled by the MPC controller.

Table 3. DC-link voltage between theoretical and simulation

Irradiation & Temperature	DC-link voltage (V)	
	Theoretical	Simulation
800 W/m^2& 35°C	70.39	71.42
500 W/m^2& 29°C	75.49	76.54
700 W/m^2& 41°C	36.00	36.15

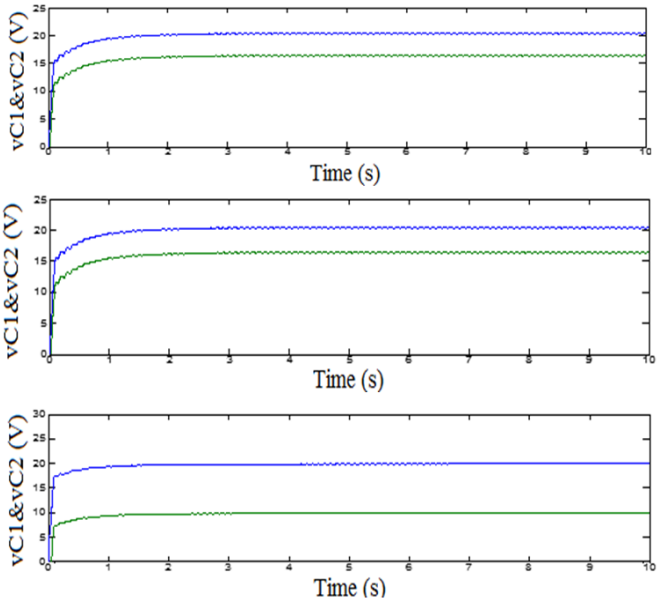

Fig. 5. Capacitors voltages of bridge module 1, 2 & 3

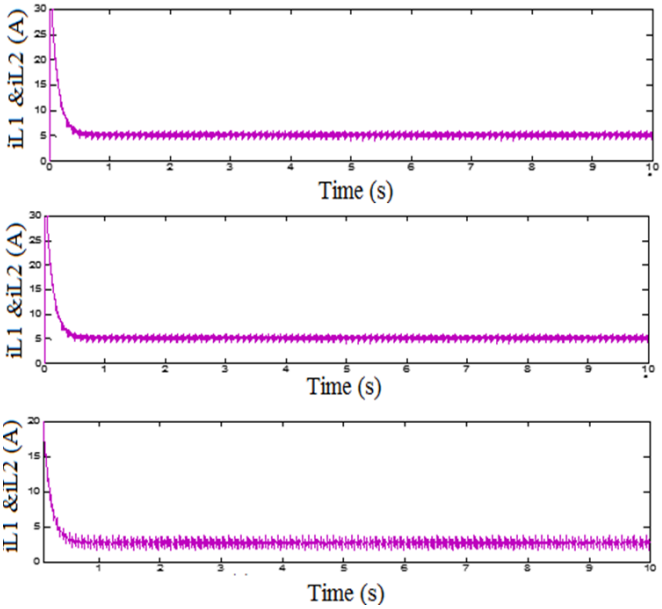

Fig. 6. Inductor current of the bridge module 1, 2 & 3

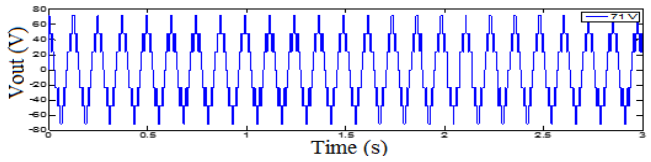

Fig. 7. Seven level staircase voltage of the QZS-CMI

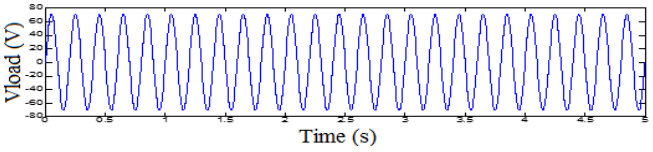

Fig. 8. The load voltage waveform of the system

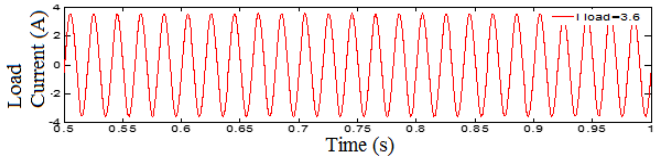

Fig. 9. Load current waveform of the system

5.1.2. Fast dynamic response analysis

The dynamic response of the MPC is observed for the change in the input voltage, the capacitor reference voltage, and the output voltage of the controlled capacitor. Here, a step-change in reference capacitor voltage at 0.4 sec and the DC voltage is varied from 24V to 32V, and the controller performance is analysed through voltage regulation of the capacitor. The system is analysed by maintaining a constant capacitor voltage, and the shoot-through duty ratio is regulated by MPC.

This method ensures that the disturbance in the input is not reflected in the DC side. By following this method, the MPC identifies the changes in capacitor reference voltage at a faster rate, and hence, it minimizes the voltage stress on the switching device.

The simulation performance of the MPC operation and PR operation is compared, and it is shown in Fig. 10 it clearly indicates that the response of PR controller is moderate as compared to MPC.

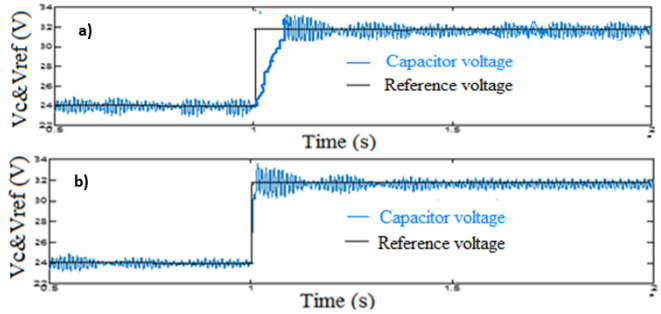

Fig. 10. A step-change in input voltage from 24V to 32V (a). PR controller; (b). MPC controller.

5.1.3. THD analysis

THD under steady-state conditions was calculated, and they are shown in Fig. 11. It shows that the THD is within the acceptable limit, i.e., it satisfies the IEEE 519 harmonic standard. The simulation results have proven that MPC has lower THD than the linear PR and PI controller. It is noted that the MPC technique has better performance in all aspects compared to the PR and PI technique [22]. The comparison between the MPC, PR and PI controllers are summarized in Table 4.

Table 4. Comparison of simulation results between proposed and existing methods

Type	MPC controller	PR controller	PI controller
Modulation technique	Not required	Required	Required
Control of Multivariable	A single control law is required.	Requires more loops	Requires more loops which make the system complex
Dynamic response	Fast response	Moderate response	Slow
I_{THD} (%)	2.17	2.64	2.86

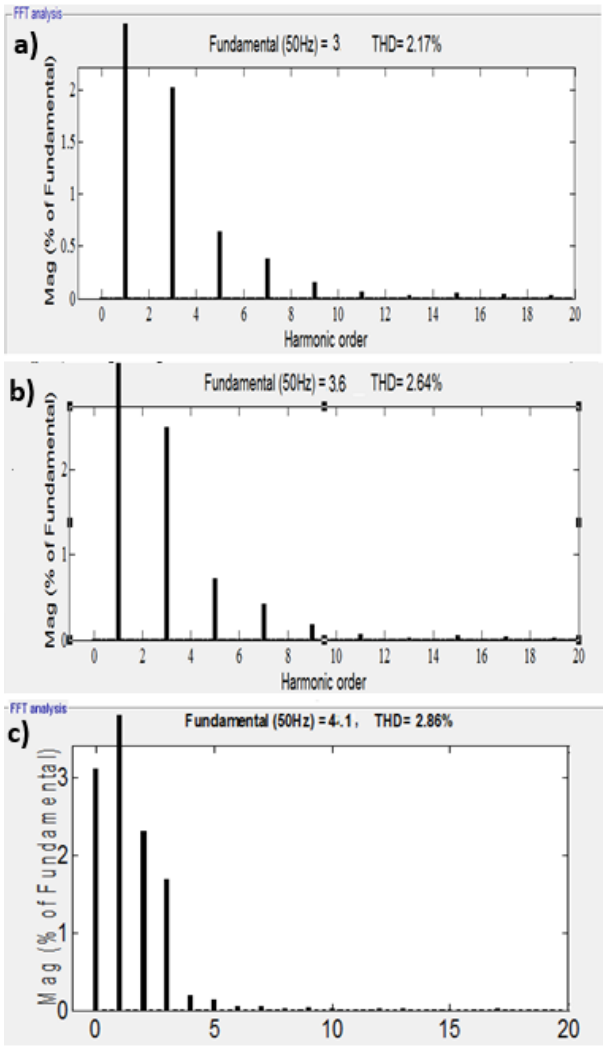

Fig. 11. THD for **(a).** MPC method; **(b).** PR controller; and **(c).** PI controller

5.2. Experimental Validation of Simulated Results

The proposed QZS-CMI for the PV system and MPC control algorithm are modeled and verified with the experimental arrangement, as shown in Fig. 12. The parameters of each module in the QZS network are alike as that of simulation data. DC voltage sensor LV20-P is used in the experimental system to measure the PV voltage in each panel. The voltage signal flows through A/D port, and the duty cycle is generated. Then, it is given to the controller with the help of the P&O block. Microcontroller (PIC16F877A) based control board controls the MPC control scheme. A 16-bit CCPR1 register is in the central part of the circuit with CCPR1L and CCPR1H registers. These registers capture and compare the binary number stored in the timer register TMR1H and TMR1L. When compares, if it is enabled by software, the timer TMR1 reset may occur. Besides, the CCP1 and CCP2 module can generate modulation index (M) and shoot-through signal (Dn), respectively. The three bridge legs with MOSFET IRF840 in the QZS-CMI system are driven by the 12 pulse gate signals from the registers.

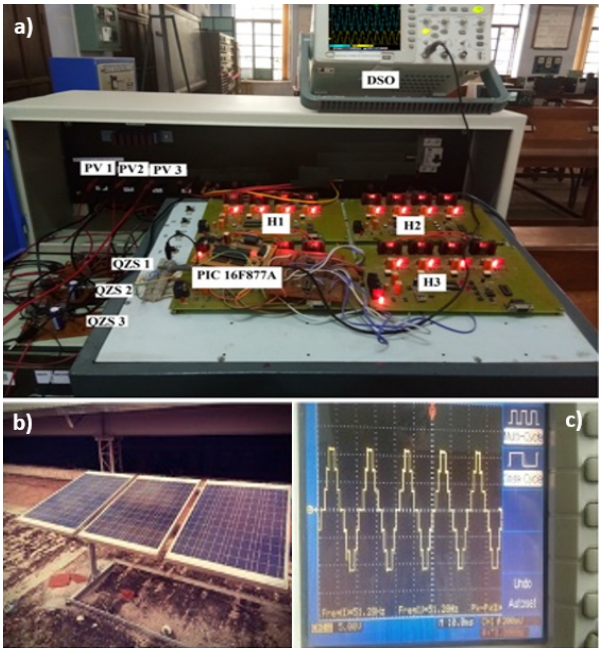

Fig. 12. Experimental setup **(a)** Entire system; **(b)** BP SX 150 W PV panel; **(c)** Seven level voltage waveform using DSO

The Capacitors C1, C2 are fixed with the same values as 300µF and the Inductors L1, L2 are fixed with the same values 500 µH. These are used to control the voltage and current ripple of the system, respectively.

The results obtained through the experimental setup are depicted in Fig. 13 and Fig. 14, which include DC link voltage and capacitors voltage waveforms. The irradiation of the PV panels is 850 W/m^2 per module, and hence, it provides the desired power of 148 W. Fig. 15 shows the inductor current waveform.

The performance of the proposed model is tested under a closed-loop operation on a resistive load of 30 Ω. The result of the experimental THD is shown in Fig. 16. The results are observed from the DSO-Scintech 7040C power meter. The proposed optimal control scheme maximizes the power transferred from PV source to the load in different light conditions and generates a nearly sinusoidal voltage with minimum harmonic distortion.

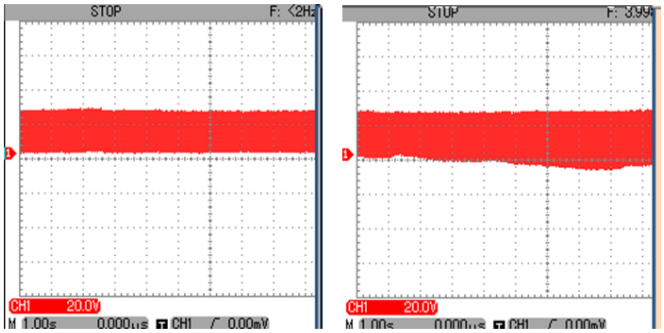

Fig. 13. Experimental results of DC-link voltage waveforms

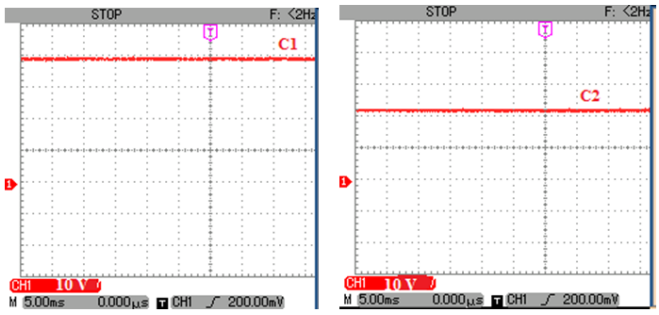

Fig. 14. Experimental results of the capacitors voltage waveforms

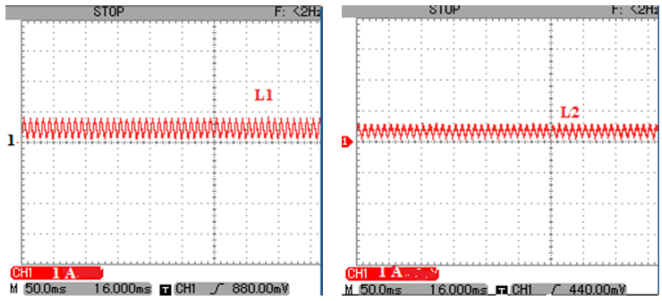

Fig. 15. Experimental results of the inductor current waveforms

Fig. 16. Experimental result of THD

6. Conclusions and Future Work

The inference from the simulation and experimental results makes clear that the QZS-CMI achieves far better performance metrics in PV based off-grid applications. The usage of the voltage sensor reduces the cost and maintenance problem. The invasion of the MPC algorithm increases the overall performance of the system formulated by the QZS-CMI inverter. The simulated results of the proposed technique were compared with the linear PR controller, which does not require any modulation process and additional control loops. This reduces the complexity controller design and also achieves a fast response. The THD values obtained from simulation and experimental results were observed as 2.17% and 2.426 % respectively, which is in the limit of the IEEE standard.

The current work deals with the change in irradiance and temperature of PV panel whereas this could also be extended by adding essential variables like partial shading parameter etc. The MPC control on QZS-CMI with PV panel is implemented with a single-phase stand-alone load and it could also be implemented in an online grid-connected power system.

References

[1] M. A. Sameh, M. A. Badr, M. I. Mare and M. A. Attia, "Enhancing the Performance of Photovoltaic Systems under Partial Shading Conditions Using Cuttlefish Algorithm," 2019 8th International Conference on Renewable Energy Research and Applications (ICRERA), Brasov, Romania, 2019, pp. 874-885. (Conference Paper)

[2] F. Ayadi, I. Colak, N. Genc and H. I. Bulbul, "Impacts of Wind Speed and Humidity on the Performance of Photovoltaic Module," 2019 8th International Conference on Renewable Energy Research and Applications (ICRERA), Brasov, Romania, 2019, pp. 229-233. (Conference Paper)

[3] A. A. Abdalla and M. Khalid, "Smoothing Methodologies for Photovoltaic Power Fluctuations," 2019 8th International Conference on Renewable Energy Research and Applications (ICRERA), Brasov, Romania, 2019, pp. 342-346. (Conference Paper)

[4] Pires, V. F., Monteiro, J., & Silva, J. F. (2019, November). A Grid-Connected PV Multilevel Cascaded Inverter System Based on Single and Three-Phase Two-Level Inverters. In 2019 8th International Conference on Renewable Energy Research and Applications (ICRERA) (pp. 118-123). (Conference Paper)

[5] Villanueva, E., Correa, P., Rodriguez, J., Pacas, M., "Control of a single-phase cascaded H-bridge multilevel inverter for grid-connected photovoltaic systems," IEEE Trans. Ind. Electron., Vol. 56, No. 11, pp. 4399-4406, 2009. (Article)

[6] Rivera, S., Kouro, S., et. al., 2011, "Cascaded H-bridge multilevel converter multistring topology for large scale photovoltaic systems. in Proc. IEEE ISIE," 1837-1844. (Conference Paper)

[7] Zhou Y, Liu L, Li, H., "A high-performance photovoltaic module-integrated converter (MIC) based on cascaded quasi-z-source inverters (qZSI) using eGaN FETs. IEEE Trans. Power Electron. Vol. 28, No. 6, pp. 2727-2738, 2013. (Article)

[8] Lingzhi, Yi., Qingzhong Gui, Zhen Wang, "A novel phase-shifted pulse width amplitude modulation for extended-boost quasi-Z source cascaded multilevel inverter based on photovoltaic power system," J. Renewable Sustainable Energy 11, 015304, 2019. (Article)

[9] Sun, D., Ge., B., Bi, D.,Peng, F., Z., "Analysis and control of quasi-Z source inverter with battery for grid-connected PV system," Inter. J. Elect. Power Energy Sys., 46, 234–240. 2013.

[10] Bajestan, M., M., Madadi, H.,Shamsinejad, M., A., "Control of a new stand-alone wind turbine-based variable speed permanent magnet synchronous generator using quasi-Z-source inverter," Elec. Power Sys. Res., 177, 106010. (2019). (Article)

[11] M Senthil Kumar, PS Manoharan, "THD mitigation in various level quasi Z-source cascaded inverter by hybrid step modulation-SHEPWM method," Journal of Elect. Eng. 17 (3), 100-109. 2017. (Article)

[12] Aamir, M., Kalwar, K. A., Mekhilef, S., "Proportional-resonant and slide mode control for single-phase ups inverter," Electric Power Components and Systems," 45(1), 11–21.2016. (Article).

[13] Prasad, S., Purwar, S., Kishor, N., "Non-linear sliding mode load frequency control in multi-area power system," Control Engineering Practice, 61, 81–92. (2017). (Article).

[14] J. Hu, J. Zhu, and D. G. Dorrell, "Model predictive control of inverters for both islanded and grid-connected operations in renewable power generations," IET Renewable Power Generation, 8(3), 240–248 (2014).

[15] Panagiotis, K., Konstantinos, P., Antonios K, Stefanos, M., "A single-phase nine-level inverter for renewable energy systems employing model predictive control," Ener. Convers. Manage. 89, 427-437.2015. (Article).

[16] Aditi C., Kanungobarada, M., Vinaya S., K., and Kishor, T., "Power quality enhancement of single phase grid tied inverters with model predictive current controller," J. Renewable Sustainable Energy, 9, 015301 (2017). (Article).

[17] Cunha, R., B., A., Inomoto, R., S., Altuna, J., A., T., Costa, F., F., Di Santo, S., G., Sguarezi Filho, A. J., "Constant switching frequency finite control set model predictive control applied to the boost converter of a photovoltaic system," Solar Energy, 189, 57–66.2019. (Article).

[18] Jabbour, N., Mademlis, C., "Online parameters estimation and auto-tuning of a discrete-time model predictive speed controller for induction motor drives," IEEE Trans. Power Electron., Vol. 34, No. 2, pp. 1548-1559, 2018. (Article)

[19] Taheri, A., Zhalebaghi, MH., "A new model predictive control algorithm by reducing the computing time of cost function minimization for NPC inverter in three-phase power grids," ISA Trans. Vol. 71, pp. 391-402, 2017. (Article)

[20] Kakosimos, P., Pavlou, K., Kladas, A., Manias, S., "Improved design of constrained model predictive tracking control for batch processes against unknown uncertainties," Energ. Converge. Manage., Vol. 89, pp. 427-437, 2015. (Article)

[21] Subudhi, B., Panda, G., "Comparison of output power control performance of wind turbine using pi, fuzzy logic and model predictive controllers," International Journal of Renewable Energy Research (IJRER), Vol. 8, No. 2, pp. 1062-1070, 2018. (Article)

[22] I. Colak, E. Kabalci and G. Keven, "The Effects of PR Control in Three-Level Single-Phase Multilevel Inverter," 2019 8th International Conference on Renewable Energy Research and Applications (ICRERA), Brasov, Romania, 2019, pp. 821-826. (Conference Paper)